HHS Public Access

Author manuscript

DNA Repair (Amst). Author manuscript; available in PMC 2017 December 01.

Published in final edited form as:

DNA Repair (Amst). 2016 December ; 48: 51–62. doi:10.1016/j.dnarep.2016.10.011.

Identification of SUMO Modification Sites in the Base Excision Repair Protein, Ntg1

Daniel B. Swartzlander[a,b,1,2], **Annie J. McPherson**[a,b,2], **Harry R. Powers**[a,3], **Kristin L. Limpose**[a,c], **Emily G. Kuiper**[a,d], **Natalya P. Degtyareva**[a,e], **Anita H. Corbett**[a,e,4], and **Paul W. Doetsch**[a,e,f,g,4]

[a]Department of Biochemistry, Emory University School of Medicine, Atlanta, GA 30322

[b]Graduate Program in Genetics and Molecular Biology, Emory University School of Medicine, Atlanta, GA 30322

[c]Graduate Program in Cancer Biology, Emory University School of Medicine, Atlanta, GA 30322

[d]Graduate Program in Biochemistry, Cell and Developmental Biology, Emory University School of Medicine, Atlanta, GA 30322

[e]Winship Cancer Institute, Emory University School of Medicine, Atlanta, GA 30322

[f]Department of Radiation Oncology, Emory University School of Medicine, Atlanta, GA 30322

[g]Department of Hematology and Medical Oncology Emory University School of Medicine, Atlanta, GA 30322

Abstract

DNA damaging agents are a constant threat to genomes in both the nucleus and the mitochondria. To combat this threat, a suite of DNA repair pathways cooperate to repair numerous types of DNA damage. If left unrepaired, these damages can result in the accumulation of mutations which can lead to deleterious consequences including cancer and neurodegenerative disorders. The base excision repair (BER) pathway is highly conserved from bacteria to humans and is primarily responsible for the removal and subsequent repair of toxic and mutagenic oxidative DNA lesions. Although the biochemical steps that occur in the BER pathway have been well defined, little is known about how the BER machinery is regulated. The budding yeast, *Saccharomyces cerevisiae* is a powerful model system to biochemically and genetically dissect BER. BER is initiated by DNA *N*-glycosylases, such as *S. cerevisiae* Ntg1. Previous work demonstrates that Ntg1 is post-

[4]To whom correspondence should be addressed. Tel: +1 404 727 0409; Fax: +1 404 727 2618; medpwd@emory.edu Address: 1510 Clifton Rd. NE RRC 4013 Atlanta, GA 30322, Correspondence may also be addressed to Anita H. Corbett. Tel: +1 404 727 4546; Fax: +1 404 727 3954; acorbe2@emory.edu Address: 1510 Clifton Rd. NE RRC 4117 Atlanta, GA 30322.

[1]Current address: Baylor College of Medicine, Houston, TX 77030

[2]Co-first author

[3]Current address: Department of Medicine, University of Florida, Gainesville, FL 32610

Conflict of Interest

The authors declare that there are no conflicts of interest.

translationally modified by SUMO in response to oxidative DNA damage suggesting that this modification could modulate the function of Ntg1. In this study, we mapped the specific sites of SUMO modification within Ntg1 and identified the enzymes responsible for sumoylating/desumoylating Ntg1. Using a non-sumoylatable version of Ntg1, ntg1ΔSUMO, we performed an initial assessment of the functional impact of Ntg1 SUMO modification in the cellular response to DNA damage. Finally, we demonstrate that, similar to Ntg1, the human homologue of Ntg1, NTHL1, can also be SUMO-modified in response to oxidative stress. Our results suggest that SUMO modification of BER proteins could be a conserved mechanism to coordinate cellular responses to DNA damage.

Keywords

Base Excision Repair (BER); Ntg1; NTHL1; SUMO; Sumoylation

Introduction

Genomes in both the nucleus and mitochondria are constantly exposed to various exogenous and endogenous DNA damaging agents (1). A suite of DNA repair pathways cooperate to ensure the efficient repair of numerous types of DNA damage that result from such exposures (2, 3). Oxidative DNA damage, caused by numerous sources including cellular metabolism (4, 5) and exogenous factors (6), is one of the most common forms of DNA damage. Estimates suggest that 90,000 oxidative lesions and 200,000 apurinic/apyrimidinic (AP) sites are generated per human cell per day (7–9). Unrepaired lesions can result in the accumulation of mutations which can trigger deleterious consequences including cancer and neurodegenerative disorders (1–3, 7, 8, 10–16). The base excision repair (BER) pathway is primarily responsible for the removal and repair of toxic and mutagenic oxidative DNA damage (3, 17–19). Numerous studies have defined in detail the biochemical steps that occur in the BER pathway (3, 20), but little is known about how the BER machinery is regulated (21).

BER is initiated by the recognition and hydrolysis of a damaged base by a DNA *N*-glycosylase leaving an AP site (3, 20, 22, 23). The AP site is then further processed to create a nick in the DNA backbone (3, 20, 22, 23). Subsequent steps create a single-strand break that is then filled by a specialized DNA polymerase and sealed by ligase (3, 20, 22, 23). These steps must occur in a sequential manner ensuring that AP sites and single strand breaks are properly managed to allow repair at the initial site of DNA damage without causing collateral damage via accumulation of BER intermediates (3, 20, 22, 23). The human NTHL1 protein, which is a bifunctional Endonuclease III–like *N*-glycosylase/AP lyase, is responsible for initiating repair of a wide array of oxidative lesions (21, 24–26). As the initiating factor in the BER pathway (3, 21, 22), NTHL1 must be regulated to ensure that repair is rapid, but also regulated to prevent the accumulation of toxic and mutagenic AP sites and single strand breaks that are the products of NTHL1 enzymatic activity (21, 24–26). *N*-glycosylase regulation could occur through a number of distinct mechanisms including modulating protein levels, protein localization, protein-protein interactions, and post-translational modifications (27–35).

Recent discoveries highlight the importance of *N*-glycosylase regulation in cancer (36, 37). Several studies identified mutations in the *NTHL1* gene in a recently characterized cancer predisposition syndrome (38–40). These heterozygous loss-of-function mutations in *NTHL1* predispose patients to colorectal cancer and other forms of cancer (38–40). Altered NTHL1 function can also result in mislocalization/accumulation of the protein in the cytoplasm of cancer cells in a subset of gastric tumors (36). These studies provide evidence that proper function of NTHL1 is critical to maintain genomic integrity and cellular homeostasis.

Much of the work that has contributed to our knowledge of DNA repair mechanisms has exploited the budding yeast *S. cerevisiae* as DNA repair pathways are conserved through evolution (41). Recent studies of the *S. cerevisiae* orthologues of NTHL1, Ntg1 and Ntg2, reveal that these proteins are post-translationally modified by the Small Ubiquitin-like MOdifier, SUMO (24, 42). The Ntg1 protein is modified in response to DNA damage (24, 42). Sumoylation has the potential to function in a number of regulatory roles including modulating protein-protein interactions and protein activity (27–35). One well-characterized example of SUMO-mediated regulation of the BER pathway is the human thymine DNA glycosylase (TDG), where sumoylation of TDG triggers a conformational change which alters the DNA binding pocket of the enzyme to influence enzyme turnover (43–45). This conformational change in TDG decreases the affinity of TDG for DNA leading to an increase in the off rate and hence an increase in the catalytic efficiency (turnover) of TDG (43, 44). Similarly, sumoylation could also modulate the function of Ntg1; however, the impact of SUMO modification on Ntg1 function has not yet been explored.

Critical to defining the functional role of SUMO modification of Ntg1 is identifying the SUMO modified sites within Ntg1. In this study, we identify the enzymes that mediate/regulate sumoylation of Ntg1. We also map the SUMO-modified sites on Ntg1 and perform an initial assessment of the functional importance of sumoylation of Ntg1. In addition, we demonstrate that, similar to Ntg1, human NTHL1 can also be SUMO-modified in response to oxidative stress. Our results suggest that SUMO modification of BER proteins could represent an evolutionarily conserved mechanism by which cells respond to oxidative DNA damage.

Materials and Methods

3.1 Strains, Plasmids, and Media

All haploid *S. cerevisiae* strains and plasmids used in this study are listed in Table 1. *S. cerevisiae* cells were cultured at 25°C, 30°C, or 37°C in YPD medium (1% yeast extract, 2% peptone, 2% dextrose, 0.005% adenine sulfate, and 2% agar for plates) or SD medium (0.17% yeast nitrogen base, 0.5% ammonium sulfate, 2% dextrose, 0.5% adenine sulfate, and 2% agar for plates). In order to introduce plasmids, cells were transformed by a modified lithium acetate method (46).

A centromeric vector (*CEN*, *URA3*), pRS316 (47) was employed as the backbone for the generation of a construct expressing C-terminally tagged Ntg1-TAP fusion protein (pD0436). The insert was amplified using the primers listed in Table 2 and inserted at the *Not*I restriction site of pRS316 (47). The insert includes the tetracycline repressible

promoter (Tet-Off) and the C-terminally tagged *NTG1-TAP* fusion from the DSC0295 strain (24). The *S. cerevisiae* haploid deletion mutant *ntg1Δ* (DSC0470) generated by dissection of tetrads derived from heterozygous diploid hDNP19 (19), and the SUMO pathway mutant collection (E3 ligase mutant strains, *siz1Δ, siz2Δ, and siz1Δ/siz2Δ* and desumoylase mutant stains *ulp1-ts* and *ulp2Δ*) were utilized to assess the level of sumoylated wildtype and mutant Ntg1 (19, 48, 49). All lysine to arginine amino acid substitutions (Supplemental Figure 1C) were created by site-directed mutagenesis performed using the QuikChange II Site-Directed Mutagenesis Kit (Stratagene) with the primers listed in Table 2. The resulting plasmids were sequenced to ensure the introduction of the desired mutation and the absence of any additional mutations.

To express recombinant Ntg1, the *NTG1* open reading frame was cloned into pET-15b (Invitrogen) to generate N-terminal His6 epitope tagged His6-Ntg1 (pD0390) (Table 1). Site-directed mutagenesis of *His6-NTG1* was performed at lysines 20, 38, 376, 388, and 396 (lysines to arginines) to create a nonsumoylatable Ntg1 (ntg1ΔSUMO), *His6-Ntg1ΔSUMO* (pD0493), and at lysine 243 (lysine to glutamine), *His6-Ntg1Δcat* (pD0394) (Table 1). Expression vectors were transformed into DE3 cells.

Site-directed mutagenesis at the endogenous *NTG1* locus of the wildtype (DSC0367) parent was performed via *delitto perfetto* protocol (50) to generate $ntg1_{K20,38,376,388,396R}$. The resulting variants were then crossed with haploid BER-Nucleotide Excision Repair- (NER-) mutants to create diploids which were then dissected to identify cells with each Ntg1 variant BER*/NER- strain (DSC0367, DSC0369, DSC0371, DSC0561).

NTHL1 was cloned from the RG214598 plasmid (Origene) using the NTHL1-Flag primer pair for the addition of the Flag-tag and cloned into the pcDNA3.1 (+) vector using the *Hin*dIII and *Bam*HI sites.

3.2 Exposure to DNA Damaging Agents

S. cerevisiae cells were grown in 5–35 mL YPD or SD -URA media to either 2×10^7 or 1×10^8 cells/mL, centrifuged, and washed with water. Cells were then resuspended in 5–35 mL water, YPD, or plated onto YPD agar plates containing the appropriate agent: 20 mM hydrogen peroxide (Sigma); or 0.005–0.3% methyl methanesulfonate (MMS) (Sigma). Cells were exposed to agents for 1–2 hours as indicated at 30°C or 37°C.

3.3 Immunoblotting Ntg1

The steady-state level of each Ntg1-TAP fusion protein variant was assessed by immunoblotting whole cell lysates with the rabbit polyclonal anti-TAP antibody (1:3,333 dilution, Open Biosystems) to determine the relative level of differentially modified Ntg1 products. An anti-3-phosphoglycerate (PGK) antibody (1:10,000 dilution; Invitrogen) was used as a control determine the relative level of protein lysate loaded into each lane.

The analysis of immunoblots was performed utilizing the ECL Plex immunoblotting detection system (Amersham), the Typhoon Trio variable mode imager (GE Healthcare), and the ImageQuant TL software package (GE Healthcare). To quantify the percentage of modified Ntg1-TAP, the ratio of modified Ntg1 bands to total Ntg1 signal (including

modified and unmodified) was determined for wildtype Ntg1 and each lysine to arginine amino acid substitution variant of Ntg1. Previous work demonstrates that modified Ntg1 contains at least one covalently linked SUMO and the size of higher bands is consistent with multiple SUMO additions(24). Standard error of the mean was calculated for each. The two-sample Student's t-test was employed to test for significance (α=0.05).

3.4 Cultured cell lines and cell culture

HT29 colon adenocarcinoma cells were cultured in McCoy's 5A modified media (Corning) and supplemented with 10% FBS, penicillin and streptomycin. Cultured cells were passaged every 3–4 days, or upon 80% confluency.

3.5 NTHL1-Flag immunoprecipitation

HT29 colon adenocarcinoma cells were seeded at a density of 1×10^6 cells in 100 cm^2 dishes. Transfection of the NTHL1-Flag construct or empty Flag vector was performed using Lipofectamine3000 (Invitrogen) and a final concentration of 10 μg plasmid/dish. The hydrogen peroxide incubation was performed with a final concentration of 125 μM hydrogen peroxide in sterile PBS for 15 minutes at 37°C. All cells were lysed in NP40 buffer (50 mM Tris pH 8.0, 100 mM NaCl, 32 mM NaF, 0.5% NP40 detergent) supplemented with protease and phosphatase inhibitors (Thermo Scientific), and SENP (de-SUMOylase) SUMO-2 aldehyde inhibitors (Enzo Life Sciences). Antibodies for Flag (Rabbit, 2368; Cell Signaling) or IgG (mouse, ab77118; abcam) were conjugated to Protein G Dynabeads (10007D; Life Sciences) for 2 hours prior to adding lysates. For each sample, 500 μg of total protein was added to the beads and rotated overnight at 4°C. Beads were washed three times in NP40 buffer for 5 minutes each. NTHL1-Flag was eluted from the beads using a 3X Flag® peptide (Sigma) for 2 hours at a working concentration of 100 μg/mL per the manufacturer's instructions.

Following Flag peptide elution, samples were added to Laemmli buffer (50% glycerol, 10% SDS, 100 mM Tris, pH 6.8), boiled for 5 minutes at 95°C, and loaded on 4–12% Bis-Tris gels (Invitrogen). Proteins were transferred onto a polyvinylidene fluoride membrane and blocked with 5% ECL prime (GE Healthcare) in 0.1% PBST for 1 hour at room temperature. Blots were incubated in primary antibodies overnight at 4°C. All washes were performed in 0.1% PBST at room temperature, and the corresponding horseradish peroxidase-conjugated secondary antibodies were added for 1 hour. Antigen-antibody complexes were detected using Supersignal™ west pico chemiluminescent substrate kit (Thermo Scientific). Antibodies used for western blotting were: NTHL1 (mouse, cat # MAB2675; R&D Systems) and SUMO-2/3 (rabbit, made in Nicholas Seyfried lab, Emory University).

3.6 Structural modeling

The Protein Homology/analogY Recognition Engine version 2.0 (Phyre2) server was used to generate a model of Ntg1 based on its *E. coli* Endonuclease III homolog (PDB ID: 2ABK). The N-terminal and C-terminal domains do not share homology with *E. coli* Endonuclease III but align to other bacterial endonucleases. The N-terminal domain aligns to the restriction endonuclease BsaW*I* (PDB ID: 4ZSF) and the C-terminal domain aligns to the endonuclease

Bgl*II* (PDB ID: 1DFM). PyMOL Molecular Graphics System, Version 1.8 Schrödinger LLC was used to model these structures.

3.7 Overexpression and purification of the recombinant Ntg1 variants for in vitro DNA strand scission assay

To assess the functional consequences of changing five lysines (K20,K38,K376,K388,K396) to arginine within Ntg1, we expressed and purified recombinant protein containing these five amino acid substitutions. We designated this recombinant protein ntg1(K->R)$_5$. As controls, we employed wildtype Ntg1 and a catalytic mutant of Ntg1 (lysine 243 to glutamine) which we term ntg1Δcat. Recombinant Ntg1 was purified as previously described (51). Briefly, *Escherichia coli* BL21 (DE3) cells containing each variant *His6-Ntg1* plasmids were grown to an OD600 of 0.5–1.0 and expression induced for 4 hours at 25°C. Cells were lysed via sonication and the supernatant was applied to Ni-NTA agarose beads purification (Qiagen) to crudely purify the His6-Ntg1 variants. Crude lysate was eluted through a gravity flow column (BIORAD) and dialyzed. Crudely purified His6-Ntg1 variants were further purified to apparent homogeneity by fast protein liquid chromatography.

3.8 Preparation of oligonucleotide and DNA strand scission assay

To assess the functional consequences of changing five lysines (K20,K38,K376,K388,K396) to arginine within Ntg1, we employed an in vitro strand scission assay. An oligonucleotide containing dihydrouracil (DHU) at position 13 (DHU-31mer) was purchased from Midland Certified Reagent Company (Midland, TX, USA). A complementary strand containing a guanine opposite the DHU position was obtained from Eurofins MWG/Operon (Huntsville, AL, USA). The DHU-31mer was 5'-end-labeled with [γ-32P] ATP (Amersham) and T4 polynucleotide kinase (Promega) prior to annealing to the complementary strand (24). Single-stranded DHU-31mer was annealed in a 1:1.6 molar ratio to the appropriate complementary strand, heated to 80°C for 10 minutes and cooled slowly to room temperature.

The AP lyase activity of purified Ntg1 variants (Ntg1, ntg1(K->R)$_5$, and ntg1Δcat) was assayed as previously described (51). Briefly, DNA strand scission assays were carried out in a standard reaction buffer (20 mL) containing 100 mM KCl, 10 mM Tris–HCl, pH 7.5, 1 mM EDTA, 50 fmol of labeled DNA substrate and 20 fmol of Ntg1 protein. Reactions were performed at 37°C for 15 minutes and then stopped by the addition of 10 μL of loading buffer (90% formamide, 1mM EDTA, 0.1% xylene cyanol and 0.1% bromophenol blue) followed by heating at 95°C for 5 minutes. Reaction products were then resolved on a denaturing-urea polyacrylamide gel (15%) and analyzed with a Typhoon Trio variable mode imager (GE Healthcare).

3.9 Functional analysis of Ntg1 in vivo

To test the sensitivity and the biological function of the Ntg1 complete sumoylation null mutant (ntg1$_{K20,38,376,388,396R}$), which we term ntg1ΔSUMO (DSC0561), to DNA damaging agents, a serial dilution and spotting assay was employed. Each strain was grown at 30°C to an OD600 of 0.3 – 0.6 in YPD, washed in 5 mL of water, and then diluted to 2×10^7 cells/mL in water. Five-fold serial dilutions of cells were then plated onto plates

containing only YPD or YPD with 0.005% MMS. Plates were incubated at 30°C and then analyzed for sensitivity at days 2 and 4.

Growth kinetics experiments were carried out using *S. cerevisiae* cells that express each Ntg1 variant encoded at the endogenous *NTG1* locus in a DNA repair compromised background (DSC0367, DSC0369, DSC0371, and DSC0561). The growth kinetics of four independently isolated ntg1ΔSUMO variants (DSC0561) and four wildtype Ntg1 (DSC0371), all in a DNA repair compromised background, were tested by analyzing growth curves. Ntg1 sumoylation mutants were grown to saturation over 2 days at 30°C in YPD. Cell concentrations were normalized by OD600, and then samples were diluted to an OD600 of 0.05 in 150 μL of YPD medium containing 0, 0.005, or 0.010% MMS and added to the wells of a 96-well microtiter plate. Cell samples were loaded in duplicate, were grown at 30°C with shaking, and absorbance at OD600 was measured every 30 minutes for 48 hours in an ELX808 Ultra microplate reader with KCjunior software (Bio-Tek Instruments, Inc.). The samples for each genotype and duplicate were averaged for every time point and differences between the two genotypes was analyzed by Students t-test.

Results

4.1 Genetic analysis of the Ntg1 sumoylation pathway

Our group has previously shown that in response to cellular exposure to hydrogen peroxide, Ntg1 is post-translationally modified by SUMO (24). As shown in Figure 1A, several Ntg1 bands are detected upon exposure to hydrogen peroxide suggesting that Ntg1 could be modified by multiple post-translational modifications, including the possibility for addition of multiple SUMO moieties. To determine whether SUMO modification of BER proteins that initiate repair is conserved, we tested whether we could detect sumoylation of human NTHL1. For this experiment, we transfected HT29 colon adenocarcinoma cells with NTHL1-Flag or an empty Flag vector. Cells were treated with hydrogen peroxide and immunoprecipitated with anti-Flag or with IgG as a control. Total lysate and bound fractions were subjected to immunoblotting to detect NTHL1 and SUMO. As shown in the top panel of Figure 1B, we detect NTHL1 in the input and NTHL1 is enriched in the bound fraction, as expected. In samples from cells treated with hydrogen peroxide, a higher molecular weight band of NTHL1 appears, suggesting a post-translational modification. Consistent with SUMO modification, a band of the same molecular weight is recognized by an anti-SUMO-2/3 antibody. The extent of modification of NTHL1 is greatly increased in response to hydrogen peroxide exposure (Figure 1B, bottom). We do not detect NTHL1 or SUMO-2/3 in the control IgG immunoprecipitation. Thus, both *S. cerevisiae* Ntg1/Ntg2 (24) and human NTHL1 can be modified by SUMO.

Sumoylation involves a series of conjugations that, in *S. cerevisiae*, are catalyzed by the E1 (Uba2/Aos1 heterodimer), the E2 (Ubc9), and one of four E3 (Siz1, Siz2, Mms21, and Zip3) ligases (52–57). These enzymes catalyze the attachment of the SUMO protein to a substrate lysine residue through formation of an isopeptide bond (52–57). Sumoylation is a dynamic process that is readily reversible by SUMO proteases, which in *S. cerevisiae* are Ulp1 and Ulp2 (58, 59).

To define the pathway by which Ntg1 is SUMO modified, we examined *S. cerevisiae* cells lacking the E3 ligases, Siz1 and Siz2, as well as Siz1/Siz2 double deletion cells (53, 60). We first examined Ntg1 sumoylation in these *siz1Δ and siz2Δ* mutant cells in response to hydrogen peroxide exposure (Figure 1C, D). In the *siz1Δ* cells, we detected reduced levels of Ntg1 sumoylation (1.5%) compared to wildtype control cells (4.7%) (Figure 1D). The level of Ntg1 sumoylation in the *siz2Δ* cells was largely unchanged (3.2%) as compared to wildtype. In the *siz1Δsiz2Δ* double mutant cells, we could not detect Ntg1 sumoylation (Figure 1C, D). These results demonstrate that Siz1 is the primary E3 ligase responsible for hydrogen peroxide–induced sumoylation of Ntg1 while Siz2 could play a minor role in Ntg1 sumoylation.

We next examined Ntg1 sumoylation in cells defective for the SUMO proteases, Ulp1 and Ulp2. The *ULP1* gene is essential so we employed a temperature sensitive mutant, *ulp1-1* (*ulp1-ts*) (61), and shifted cells to 37°C to inactivate Ulp1. The levels of hydrogen peroxide–induced Ntg1 sumoylation in the *ulp1-ts* mutant were significantly higher than in the wildtype control cells. The *ulp1-ts* mutant cells displayed 10.9% monosumoylated Ntg1, contrasting with 4.7% monosumoylated Ntg1 detected in the wildtype cells (Figure 1C, D). In contrast to the *ulp1-ts* cells, *ulp2Δ* cells exhibit no detectable change in sumoylation in response to hydrogen peroxide exposure when compared to wildtype (Figure 1D). These results suggest that Ulp1 serves as the primary de-sumoylase for Ntg1.

Sumoylation is a dynamic process where only a very small percent of sumoylated product is present at any given time (35). In fact, in wildtype cells, without exogenous exposure to reactive oxygen species (ROS) or oxidative stress, we do not detect modification of Ntg1 (Figure 1A). To determine whether Ntg1 is modified only in response to hydrogen peroxide or is endogenously modified at low levels, we examined Ntg1 sumoylation in the *ulp1-ts* cells and the *ulp2Δ* mutant cells in the absence of any treatment. Loss of Ulp1 function resulted in a dramatic increase in both monosumoylated and multi-modified Ntg1 compared to wildtype (Figure 1E, F). In contrast, loss of Ulp2 had no impact on Ntg1 sumoylation levels. These data indicate that Ntg1 can be sumoylated in the absence of exogenous stress.

4.2 Identification of Ntg1 sumoylation sites

Sumoylation occurs on lysine residues, typically within SUMO consensus sequences (62, 63). More than two-thirds of known SUMO substrates contain at least one consensus sumoylation motif Ψ-K-x-D/E (where Ψ is a hydrophobic residue, K is the lysine conjugated to SUMO, x is any amino acid, and D/E is an acidic residue) (62, 63). We used freely available search engines to identify predicted sumoylation sites in both NTHL1 and Ntg1 (Supplemental Figure 1A, B). Prediction software identified multiple candidate sumoylation sites in NTHL1 (Supplemental Figure 1A). To identify candidate sumoylation sites in Ntg1, we used a combination of five SUMO prediction programs: SUMOsp 1.0 (64), SUMOsp 2.0/GPS-SUMO (65, 66), SUMOplot (http://www.abgent.com/sumoplot), SUMOpre (67), and PCI-SUMO (68) This analysis identified five putative consensus sumoylation sites (K20, K38, K376, K388, K396) within Ntg1 (Figure 2A and Supplemental Figure 1B). Five putative non-consensus sumoylation sites were also identified (Figure 2A

and Supplemental Figure 1B). Consensus and non-consensus motifs of identified putative sumoylation sites and prediction scores are shown in Supplemental Figure 1B.

We initially tested for SUMO modification within these sites on Ntg1 via mass spectrometry. However, when we analyzed the bacterially expressed Ntg1 through mass spectrometry the peptides containing the putative SUMO modification sites were not detected. As an alternative approach, to determine which of these putative sites are sumoylated and to generate a form of Ntg1 that cannot be sumoylated, we performed site-directed mutagenesis to create conservative amino acid substitutions of the ten putative sumoylation site lysines to arginines. These substitutions were made in order of predicted site strength for all single sites (Supplemental Figure 1C). In total, we created 25 single and combination lysine to arginine substitutions beginning with a single substitution and proceeding with double, triple, etc. substitutions (Supplemental Figure 1C). We then analyzed the sumoylation status of all the resulting variants of Ntg1 in response to hydrogen peroxide.

The single lysine to arginine substitutions were tested first and the results showed that all Ntg1 variants containing single lysine to arginine substitutions can still be sumoylated (Figure 2B). Quantification of the single substitution data showed that one substitution examined (K396) results in a detectable decrease in the amount of monosumoylated Ntg1, suggesting that K396 could be the primary site of monosumoylation (Figure 2C). The finding that no single lysine to arginine substitution leads to a complete loss of SUMO modification supports our earlier results suggesting that Ntg1 is sumoylated at multiple lysines simultaneously. Thus, multiple substitutions are required to produce a variant that cannot be sumoylated. Single substitution of the five putative non-consensus sumoylation sites (K157, 194, 255, 359, 364) did not alter levels of Ntg1 sumoylation, indicating that these sites are not essential for Ntg1 sumoylation. Next, we tested a series of combinations of lysine to arginine Ntg1 variants for sumoylation. The double and triple mutant proteins involving the N- and C-termini, $Ntg1_{K20,38R}$-TAP and $Ntg1_{K20,38,376R}$-TAP, can both still be sumoylated (Figure 2B, C). The quadruple mutant protein, $Ntg1_{K20,38,376,388R}$-TAP, shows only a single sumoylated species; while an additional K396 to arginine substitution, leads to the complete loss of all detectable SUMO-modification of Ntg1 (ntg1ΔSUMO). For the collection of variants, changes in the levels of Ntg1 sumoylation were quantified and are presented in Table 3. These results demonstrate that Ntg1 is sumoylated at any of five consensus sumoylation sites and that all five sites must be simultaneously changed to arginine to generate an Ntg1 variant that cannot be modified by SUMO. Supplemental Figure 1C shows all of the combinations of Ntg1 variants generated and summarizes the total sumoylation loss. Thus, we have identified the five lysine residues within Ntg1 that can be sumoylated.

The lysines within Ntg1 that can be sumoylated reside in the N- and C-terminal domains that are specific to the eukaryotic enzyme and outside of the 307 residues which comprise the evolutionarily-conserved catalytic core with homology to the bacterial Endonuclease III protein (69). To provide insight into the location of these lysines within the three-dimensional structure of Ntg1, we generated a homology model of *S. cerevisiae* Ntg1 (Figure 3A) using the Protein Homology/analogY Recognition Engine version 2.0 (Phyre2) (70). The predicted model (Figure 3A) is based on the structure of the *E. coli* Endonuclease

III protein (PDB ID: 2ABK). Tan regions display the high confidence (90%) homology mapping of the region of Ntg1 (amino acids 95–335) with homology to Endonuclease III (Figure 2A). The magenta and green regions correspond to the N-terminal (amino acids 1–94) and C-terminal (amino acids 335–399) domains, respectively (Figure 2A). Although the N- and C-terminal domains of Ntg1 do not align to Endonuclease III, they are modeled based on homology to other endonucleases. The N-terminal domain aligns to the restriction endonuclease BsaW*I* (PDB ID: 4ZSF) and the C-terminal domain aligns to the endonuclease Bgl*II* (PDB ID: 1DFM). Based on our homology model (Figure 3A), the five lysines that we defined as SUMO modification sites are all surface exposed, consistent with being accessible for modification.

As sumoylation influences DNA binding and turnover of TDG (43–45), we analyzed the proximity of the sumoylation sites to the DNA binding and catalytic centers in our Ntg1 model. The structure of sumoylated-TDG (PDB ID: 1WYW) shows the close proximity of the SUMO modification to the DNA binding and catalytic site of TDG (71), illustrating why sumoylation of TGD might influence TGD catalysis. To assess whether sumoylation could impact DNA binding or catalysis by Ntg1, we superimposed our model of Ntg1 with the structure of Endonuclease III (Figure 3A). Previous work implicated K120 and D138 in catalysis and K191 in DNA binding of Endonuclease III (Figure 3A) (69). We identified the analogous amino acids in our model of Ntg1 (Figure 3A, B). Loop residues in Endo III corresponding to residues 314–318 in Ntg1 are important for DNA binding (Figure 3B). Both the catalytic residues and the DNA binding loop in Ntg1 are distant from the sumoylated lysines and extend from the opposite face of the protein. This analysis suggests that sumoylation is unlikely to directly influence Ntg1-mediated catalysis.

4.3 *In vitro* functional analysis of the nonsumoylatable Ntg1 variant, ntg1$_{K20,38,376,388,396R}$ (ntg1(K->R)$_5$)

Although changing a lysine residue to an arginine residue conserves the charge and size of the amino acid, such modest changes could induce a conformational change potentially impacting function. To address whether the conservative substitution of the five lysines that constitute the Ntg1 sumoylation sites (K20, K38, K376, K388, K396) impacts the catalytic activity of Ntg1 *in vitro*, we employed an *in vitro* oligonucleotide cleavage assay to compare the enzymatic activity of wildtype Ntg1 to ntg1$_{K20,38,376,388,396R}$, which we designate ntg1(K->R)$_5$. The oligonucleotide substrate contains dihydrouracil (DHU) which is an Ntg1 substrate (72). As a control, we employed a catalytically inactive Ntg1 (ntg1Δcat) variant created by changing the catalytic lysine at position 243 to glutamine (73). We incubated purified recombinant His6-Ntg1 variants with the oligonucleotide containing the Ntg1 substrate and detected Ntg1 enzymatic activity as cleavage of the oligonucleotide at the position of the DHU (26). As shown in the cleavage assay presented in Figure 4B, His6-ntg1(K->R)$_5$ shows enzymatic activity comparable to wildtype His6-Ntg1 whereas a catalytically inactive form of Ntg1, His6-ntg1Δcat, did not cleave the substrate. We quantitated the results of three independent cleavage experiments (Figure 4C). These results confirm that there is no difference in the activity of ntg1(K->R)$_5$ compared to wildtype Ntg1 in this assay. These results indicate that changing the five SUMO modification sites from lysine to arginine does not alter the enzymatic activity of Ntg1.

4.4 Functional analysis of Ntg1 *in vivo*

Previous studies showed that Ntg1 is SUMO–modified in response to treatment with hydrogen peroxide (24). To assess whether other types of DNA damage can induce Ntg1 sumoylation, cells were exposed to methyl methanesulfonate (MMS), which induces alkylating DNA damage (74, 75). As shown in Figure 5A, Ntg1 is sumoylated in response to treatment with MMS. We exploited this observation to examine how cells that express an Ntg1 variant that cannot be modified by SUMO ($ntg1_{K20,38,376,388,396R}$), which we designate ntg1ΔSUMO, respond to DNA damage. For these experiments, Ntg1 or ntg1ΔSUMO was expressed either in base excision and nucleotide excision repair (NER)-proficient wildtype cells (WT) or repair-deficient (*ntg1*Δ*ntg2*Δ*apn1*Δ*rad1*Δ) cells, which lack BER and NER (B-/N-) (19, 76). Cells were exposed to MMS and the growth characteristics of these cells expressing wildtype Ntg1 were compared to those expressing ntg1ΔSUMO. We then examined growth in the absence or presence of MMS (Figure 5B). Growth was analyzed at days 2 and 4 following serial dilution and spotting on plates. As expected (76), the repair proficient (WT) cells grew well under all conditions tested, regardless of which Ntg1 variant was expressed. In contrast, the repair-deficient cells display slow growth in the presence of MMS even with wildtype *NTG1*. The repair-deficient *ntg1Δ* cells were extremely sensitive to MMS (Figure 5B). Surprisingly, the *ntg1ΔSUMO* cells were less sensitive to MMS compared to cells with wildtype *NTG1*. This result suggests that sumoylation of Ntg1 could be important for coordinating DNA repair with cell cycle progression or DNA damage response.

To further examine the growth of the *ntg1ΔSUMO* cells following treatment with MMS, growth curves were generated for wildtype, repair-deficient cells, Ntg1 in repair-deficient cells, and ntg1ΔSUMO in repair-deficient cells grown in YPD with and without MMS (Figure 5C, D). The results indicate that repair-deficient cells that express ntg1ΔSUMO emerge from lag-phase earlier than repair-deficient cells expressing wildtype Ntg1 (Figure 5D). As expected, repair-deficient cells expressing either Ntg1 or ntg1ΔSUMO grew equally well in the absence of MMS (Figure 5C). These data further suggest that the sumoylation of Ntg1 plays a role in coordinating the growth arrest that occurs in response to DNA damage.

Discussion

We report here that SUMO modification is a conserved post-translational modification of *S. cerevisiae* Ntg1 and the human orthologue, NTHL1. In *S. cerevisiae*, we identified the two SUMO ligases, Siz1 and Siz2, and the desumoylase, Ulp1, critical for reversible regulation of this modification. We mapped the sites of SUMO modification in Ntg1 and created an Ntg1 that cannot be SUMO modified. Our preliminary analysis of this non-sumoylatable form of Ntg1 reveals that SUMO modification may be important for proper cellular response to DNA damage.

We identified Ulp1 as the primary desumoylase for Ntg1 with little impact of Ulp2. As the primary role of Ulp2 is to remove SUMO from poly(SUMO) chains (55), and we detect no change in SUMO modification of Ntg1 in *ulp2Δ* mutant cells (Figure 1C, D), we speculate that Ntg1 could be modified by multiple independent SUMOs rather than a single chain of multiple SUMOs. This model is consistent with our finding that five different lysine residues

in Ntg1 can be modified by SUMO. While we cannot rule out the possibility that the Ntg1-TAP used in this study is also modified by other post-translational modifications, the band shifts are consistent with the molecular size and charge of multiple SUMO molecules. Consistent with a possible role for additional post-translational modifications, mass spec analysis reveals that Ntg1 serine 71 is phosphorylated (77). Regardless, the data presented here in combination with our previous publication (24) show that Ntg1 is SUMO modified by at least one SUMO molecule and that there are at least five lysines on Ntg1 that can be SUMO modified. These SUMO molecules could coordinate other post-translational modifications.

Our data show that both hydrogen peroxide and MMS can induce sumoylation of Ntg1 (24). Like hydrogen peroxide, treatment with MMS can cause oxidative stress and generate ROS (78). Therefore, we cannot yet clearly distinguish whether hydrogen peroxide and MMS trigger sumoylation of Ntg1 through the same or distinct mechanisms. Further work will be required to determine how the sumoylation machinery responds to DNA damage and/or oxidative stress. Regulation could occur through activation of SUMO E3 ligases or through inhibition of the Ulp1 desumoylase. Further analysis will be required to dissect this mechanism.

Sumoylation can influence numerous functions of a protein including catalytic activity, localization, stability, and/or protein-protein interactions (79). As sumoylation plays a role in regulating the binding capabilities of TDG by modulating the interaction with DNA, sumoylation could also impact the DNA binding ability of Ntg1. However, based on homology modeling and mapping of the sumoylation sites, our model suggests that sumoylation at any of the five sites we identified likely does not directly interfere with the DNA binding to Ntg1. Consistent with this result, none of the Ntg1 lysine to arginine substitutions altered catalytic activity of the recombinant protein *in vitro* (Figure 4). With respect to localization, Ntg1 sumoylation at K20 and K38 on Ntg1 are within or just adjacent to the consensus organelle targeting localization sequences. The N-terminus of Ntg1 contains a mitochondrial targeting sequence (MTS) at amino acids 1–26 and a classical bipartite nuclear localization signal (cNLS) at amino acids 14–17 and 31–37 (51). The proximity of the sumoylation sites, specifically K20 and K38, to these localization signals suggests a potential role for sumoylation in regulating subcellular localization of Ntg1. In fact, our previous biochemical fractionation studies showed that sumoylated Ntg1 is detected only in the nucleus (24). Consistent with a conserved regulatory model, human NTHL1 also contains putative SUMO sites at K56 and K60 that overlap a predicted cNLS at amino acids 56–60 (Supplemental Figure 1A). Another possible function of sumoylation is to modulate proteinprotein interactions (79). Little is known about the interacting partners of Ntg1. One high-throughput yeast two-hybrid study identified two DNA damage response proteins, Rad59 and Rfc2, as physical interactors of Ntg1 (80). Rad59 is involved in double strand break repair (81), and Rfc2 is part of the ATPase clamp loader for the proliferating cell nuclear antigen (PCNA) processivity factor for DNA polymerases (82). As both of these proteins are implicated in DNA damage response, they could mediate crosstalk between BER and the DNA damage response pathway. A critical next step in understanding the functional impact of sumoylation on Ntg1 is to identify SUMO-dependent interacting proteins.

Our data (Figure 5B, C, D) show cells expressing ntg1ΔSUMO display more rapid growth compared to cells expressing wildtype Ntg1 in a DNA repair deficient background in response to MMS. Alkylation damage induced by MMS can be mutagenic and lead to cytotoxic blockage of replication forks (75, 83, 84). One possibility is that sumoylation of Ntg1 is required for proper checkpoint activation or maintenance. Cell cycle checkpoints are activated by sensor proteins, such as Rad9 (85), detecting an increase in DNA damage and initiating a signal cascade that ultimately leads to activation of Rad53, the protein kinase responsible for cell cycle arrest (86, 87). Activation of Rad53 is critical for stabilization of replication forks and activating the DNA repair pathway (81). Interestingly, improper activation of Rad53 results in an increased resistance to MMS via engagement of translesion synthesis (TLS) (88). Further investigation of this potential connection between the DNA checkpoint protein, Rad53, and the BER protein, Ntg1, could reveal a novel DNA damage response activator.

A number of studies have identified roles for SUMO in modulating DNA repair (89–98). The work presented here suggests SUMO-mediated regulation could extend to the evolutionarily conserved BER pathway. Indeed regulation of the initial step of the BER pathway could be crucial to ensure genome integrity.

Supplementary Material

Refer to Web version on PubMed Central for supplementary material.

Acknowledgments

We would like to thank Christine Dunham for her help with the generation of the protein homology model. We would also like to acknowledge members of the Corbett and Doetsch laboratories for helpful discussions and advice.

This study was supported in part by the Emory Integrated Genomics Core (EIGC), which is subsidized by the Emory University School of Medicine and is one of the Emory Integrated Core Facilities. Additional support was provided by the National Center for Advancing Translational Sciences of the National Institutes of Health under Award Number UL1TR000454. The content is solely the responsibility of the authors and does not necessarily reflect the official views of the National Institutes of Health.

Funding Sources

This work was supported by the National Institutes of General Medical Sciences [RO1 GM05872816; T32 GM008490 22; and F31 GM115178 01] and the National Institutes of Health [NIH ES011163].

References

1. Altieri F, Grillo C, Maceroni M, Chichiarelli S. DNA damage and repair: from molecular mechanisms to health implications. Antioxid Redox Signal. 2008; 10(5):891–937. [PubMed: 18205545]
2. Fortini P, Pascucci B, Parlanti E, D'Errico M, Simonelli V, Dogliotti E. The base excision repair: mechanisms and its relevance for cancer susceptibility. Biochimie. 2003; 85(11):1053–1071. [PubMed: 14726013]
3. Boesch P, Weber-Lotfi F, Ibrahim N, Tarasenko V, Cosset A, Paulus F, et al. DNA repair in organelles: Pathways, organization, regulation, relevance in disease and aging. Biochim Biophys Acta. 2011; 1813(1):186–200. [PubMed: 20950654]
4. Kryston TB, Georgiev AB, Pissis P, Georgakilas AG. Role of oxidative stress and DNA damage in human carcinogenesis. Mutation research. 2011; 711(1–2):193–201. [PubMed: 21216256]

5. Pan Y. Mitochondria, reactive oxygen species, and chronological aging: a message from yeast. Experimental gerontology. 2011; 46(11):847–852. [PubMed: 21884780]
6. de Gruijl FR, van Kranen HJ, Mullenders LH. UV-induced DNA damage, repair, mutations and oncogenic pathways in skin cancer. J Photochem Photobiol B. 2001; 63(1–3):19–27. [PubMed: 11684448]
7. Fraga CG, Shigenaga MK, Park JW, Degan P, Ames BN. Oxidative damage to DNA during aging: 8-hydroxy-2'-deoxyguanosine in rat organ DNA and urine. Proc Natl Acad Sci U S A. 1990; 87(12): 4533–4537. [PubMed: 2352934]
8. Nakamura J, Swenberg JA. Endogenous apurinic/apyrimidinic sites in genomic DNA of mammalian tissues. Cancer Res. 1999; 59(11):2522–2526. [PubMed: 10363965]
9. Salmon TB, Evert BA, Song B, Doetsch PW. Biological consequences of oxidative stress-induced DNA damage in *Saccharomyces cerevisiae*. Nucleic Acids Res. 2004; 32(12):3712–3723. [PubMed: 15254273]
10. Stefl S, Nishi H, Petukh M, Panchenko AR, Alexov E. Molecular mechanisms of disease-causing missense mutations. J Mol Biol. 2013; 425(21):3919–3936. [PubMed: 23871686]
11. Evert BA, Salmon TB, Song B, Jingjing L, Siede W, Doetsch PW. Spontaneous DNA damage in *Saccharomyces cerevisiae* elicits phenotypic properties similar to cancer cells. J Biol Chem. 2004; 279(21):22585–22594. [PubMed: 15020594]
12. Beckman KB, Ames BN. Oxidative decay of DNA. J Biol Chem. 1997; 272(32):19633–19636. [PubMed: 9289489]
13. Wallace DC. Diseases of the mitochondrial DNA. Annu Rev Biochem. 1992; 61:1175–1212. [PubMed: 1497308]
14. Wei YH. Oxidative stress and mitochondrial DNA mutations in human aging. Proc Soc Exp Biol Med. 1998; 217(1):53–63. [PubMed: 9421207]
15. Cooke MS, Evans MD, Dizdaroglu M, Lunec J. Oxidative DNA damage: mechanisms, mutation, and disease. FASEB J. 2003; 17(10):1195–1214. [PubMed: 12832285]
16. Lenaz G. Role of mitochondria in oxidative stress and ageing. Biochim Biophys Acta. 1998; 1366(1–2):53–67. [PubMed: 9714734]
17. Muftuoglu M, de Souza-Pinto NC, Dogan A, Aamann M, Stevnsner T, Rybanska I, et al. Cockayne syndrome group B protein stimulates repair of formamidopyrimidines by NEIL1 DNA glycosylase. J Biol Chem. 2009; 284(14):9270–9279. [PubMed: 19179336]
18. Larsen NB, Rasmussen M, Rasmussen LJ. Nuclear and mitochondrial DNA repair: similar pathways? Mitochondrion. 2005; 5(2):89–108. [PubMed: 16050976]
19. Degtyareva NP, Chen L, Mieczkowski P, Petes TD, Doetsch PW. Chronic oxidative DNA damage due to DNA repair defects causes chromosomal instability in *Saccharomyces cerevisiae*. Mol Cell Biol. 2008; 28(17):5432–5445. [PubMed: 18591251]
20. Sentürker S, Auffret van der Kemp P, You HJ, Doetsch PW, Dizdaroglu M, Boiteux S. Substrate specificities of the Ntg1 and Ntg2 proteins of *Saccharomyces cerevisiae* for oxidized DNA bases are not identical. Nucleic Acids Res. 1998; 26(23):5270–5276. [PubMed: 9826748]
21. Swartzlander, DB.; Bauer, NC.; Corbett, AH.; Doetsch, PW. Chapter 5 – Regulation of base excision repair in eukaryotes by dynamic localization strategies. In: Doetsch, PW., editor. Mechanisms of DNA Repair. Progress in Molecular Biology and Translational Science. Vol. 110. Oxford, UK: Academic Press; 2012. p. 93-121.
22. Nilsen H, Krokan HE. Base excision repair in a network of defence and tolerance. Carcinogenesis. 2001; 22(7):987–998. [PubMed: 11408341]
23. Memisoglu A, Samson L. Base excision repair in yeast and mammals. Mutat Res. 2000; 451(1–2): 39–51. [PubMed: 10915864]
24. Griffiths LM, Swartzlander D, Meadows KL, Wilkinson KD, Corbett AH, Doetsch PW. Dynamic compartmentalization of base excision repair proteins in response to nuclear and mitochondrial oxidative stress. Mol Cell Biol. 2009; 29(3):794–807. [PubMed: 19029246]
25. Ikeda S, Kohmoto T, Tabata R, Seki Y. Differential intracellular localization of the human and mouse endonuclease III homologs and analysis of the sorting signals. DNA Repair (Amst). 2002; 1(10):847–854. [PubMed: 12531031]

26. You HJ, Swanson RL, Harrington C, Corbett AH, Jinks-Robertson S, Sentürker S, et al. *Saccharomyces cerevisiae* Ntg1p and Ntg2p: broad specificity *N*-glycosylases for the repair of oxidative DNA damage in the nucleus and mitochondria. Biochemistry. 1999; 38(35):11298–11306. [PubMed: 10471279]
27. Bettermann K, Benesch M, Weis S, Haybaeck J. SUMOylation in carcinogenesis. Cancer Lett. 2012; 316(2):113–125. [PubMed: 22138131]
28. Cremona CA, Sarangi P, Zhao X. Sumoylation and the DNA damage response. Biomolecules. 2012; 2(3):376–388. [PubMed: 24926426]
29. Bartek J, Hodny Z. SUMO boosts the DNA damage response barrier against cancer. Cancer Cell. 2010; 17(1):9–11. [PubMed: 20129245]
30. Johnson ES. Protein modification by SUMO. Annu Rev Biochem. 2004; 73:355–382. [PubMed: 15189146]
31. Dery U, Masson JY. Twists and turns in the function of DNA damage signaling and repair proteins by post-translational modifications. DNA Repair (Amst). 2007; 6(5):561–577. [PubMed: 17258515]
32. Dou H, Huang C, Van Nguyen T, Lu LS, Yeh ET. SUMOylation and de-SUMOylation in response to DNA damage. FEBS Lett. 2011; 585(18):2891–2896. [PubMed: 21486569]
33. Thompson LH. Recognition, signaling, and repair of DNA double-strand breaks produced by ionizing radiation in mammalian cells: The molecular choreography. Mutation Research/Reviews in Mutation Research. 2012; 751(2):158–246.
34. Kirkin V, Dikic I. Role of ubiquitin- and Ubl-binding proteins in cell signaling. Curr Opin Cell Biol. 2007; 19(2):199–205. [PubMed: 17303403]
35. Bergink S, Jentsch S. Principles of ubiquitin and SUMO modifications in DNA repair. Nature. 2009; 458(7237):461–467. [PubMed: 19325626]
36. Goto M, Shinmura K, Igarashi H, Kobayashi M, Konno H, Yamada H, et al. Altered expression of the human base excision repair gene *NTH1* in gastric cancer. Carcinogenesis. 2009; 30(8):1345–1352. [PubMed: 19414504]
37. Koketsu S, Watanabe T, Nagawa H. Expression of DNA repair protein: MYH, NTH1, and MTH1 in colorectal cancer. Hepatogastroenterology. 2004; 51(57):638–642. [PubMed: 15143881]
38. Short E, Thomas LE, Hurley J, Jose S, Sampson JR. Inherited predisposition to colorectal cancer: towards a more complete picture. J Med Genet. 2015; 52(12):791–796. [PubMed: 26297796]
39. Rivera B, Castellsague E, Bah I, van Kempen LC, Foulkes WD. Biallelic NTHL1 Mutations in a Woman with Multiple Primary Tumors. The New England journal of medicine. 2015; 373(20): 1985–1986. [PubMed: 26559593]
40. Weren RD, Ligtenberg MJ, Kets CM, de Voer RM, Verwiel ET, Spruijt L, et al. A germline homozygous mutation in the base-excision repair gene NTHL1 causes adenomatous polyposis and colorectal cancer. Nature genetics. 2015; 47(6):668–671. [PubMed: 25938944]
41. Bauer NC, Corbett AH, Doetsch PW. The current state of eukaryotic DNA base damage and repair. Nucleic Acids Res. 2015; 43(21):10083–10101. [PubMed: 26519467]
42. Hannich JT, Lewis A, Kroetz MB, Li SJ, Heide H, Emili A, et al. Defining the SUMO-modified proteome by multiple approaches in Saccharomyces cerevisiae. J Biol Chem. 2005; 280(6):4102–4110. [PubMed: 15590687]
43. Hardeland U, Steinacher R, Jiricny J, Schar P. Modification of the human thymine-DNA glycosylase by ubiquitin-like proteins facilitates enzymatic turnover. EMBO JOURNAL. 2002; 21(6):1456–1464. [PubMed: 11889051]
44. Smet-Nocca C, Wieruszeski JM, Leger H, Eilebrecht S, Benecke A. SUMO-1 regulates the conformational dynamics of thymine-DNA glycosylase regulatory domain and competes with its DNA binding activity. BMC Biochem. 2011; 12:4. [PubMed: 21284855]
45. Steinacher R, Schar P. Functionality of human thymine DNA glycosylase requires SUMO-regulated changes in protein conformation. Curr Biol. 2005; 15(7):616–623. [PubMed: 15823533]
46. Ito H, Fukuda Y, Murata K, Kimura A. Transformation of intact yeast cells treated with alkali cations. J Bacteriol. 1983; 153(1):163–168. [PubMed: 6336730]

47. Sikorski RS, Hieter P. A system of shuttle vectors and yeast host strains designed for efficient manipulation of DNA in *Saccharomyces cerevisiae*. Genetics. 1989; 122(1):19–27. [PubMed: 2659436]
48. Parikh SS, Mol CD, Slupphaug G, Bharati S, Krokan HE, Tainer JA. Base excision repair initiation revealed by crystal structures and binding kinetics of human uracil-DNA glycosylase with DNA. Embo J. 1998; 17(17):5214–5226. [PubMed: 9724657]
49. Tang CH, Wei W, Liu L. Regulation of DNA repair by S-nitrosylation. Biochim Biophys Acta. 2012; 1820(6):730–735. [PubMed: 21571039]
50. Storici F, Resnick MA. The *delitto perfetto* approach to in vivo site-directed mutagenesis and chromosome rearrangements with synthetic oligonucleotides in yeast. Methods Enzymol. 2006; 409:329–345. [PubMed: 16793410]
51. Swartzlander DB, Griffiths LM, Lee J, Degtyareva NP, Doetsch PW, Corbett AH. Regulation of base excision repair: Ntg1 nuclear and mitochondrial dynamic localization in response to genotoxic stress. Nucleic Acids Res. 2010; 38(12):3963–3974. [PubMed: 20194111]
52. Sampson DA, Wang M, Matunis MJ. The small ubiquitin-like modifier-1 (SUMO-1) consensus sequence mediates Ubc9 binding and is essential for SUMO-1 modification. J Biol Chem. 2001; 276(24):21664–21669. [PubMed: 11259410]
53. Johnson ES, Gupta AA. An E3-like factor that promotes SUMO conjugation to the yeast septins. Cell. 2001; 106(6):735–744. [PubMed: 11572779]
54. Johnson ES, Blobel G. Ubc9p is the conjugating enzyme for the ubiquitin-like protein Smt3p. J Biol Chem. 1997; 272(43):26799–26802. [PubMed: 9341106]
55. Bylebyl GR, Belichenko I, Johnson ES. The SUMO isopeptidase Ulp2 prevents accumulation of SUMO chains in yeast. The Journal of biological chemistry. 2003; 278(45):44113–44120. [PubMed: 12941945]
56. Tatham MH, Jaffray E, Vaughan OA, Desterro JM, Botting CH, Naismith JH, et al. Polymeric chains of SUMO-2 and SUMO-3 are conjugated to protein substrates by SAE1/SAE2 and Ubc9. J Biol Chem. 2001; 276(38):35368–35374. [PubMed: 11451954]
57. Cheng CH, Lo YH, Liang SS, Ti SC, Lin FM, Yeh CH, et al. SUMO modifications control assembly of synaptonemal complex and polycomplex in meiosis of Saccharomyces cerevisiae. Genes Dev. 2006; 20(15):2067–2081. [PubMed: 16847351]
58. Li SJ, Hochstrasser M. A new protease required for cell-cycle progression in yeast. Nature. 1999; 398(6724):246–251. [PubMed: 10094048]
59. Li SJ, Hochstrasser M. The yeast ULP2 (SMT4) gene encodes a novel protease specific for the ubiquitin-like Smt3 protein. Mol Cell Biol. 2000; 20(7):2367–2377. [PubMed: 10713161]
60. Schwienhorst I, Johnson ES, Dohmen RJ. SUMO conjugation and deconjugation. Molecular & general genetics : MGG. 2000; 263(5):771–786. [PubMed: 10905345]
61. Soustelle C, Vernis L, Freon K, Reynaud-Angelin A, Chanet R, Fabre F, et al. A new Saccharomyces cerevisiae strain with a mutant Smt3-deconjugating Ulp1 protein is affected in DNA replication and requires Srs2 and homologous recombination for its viability. Molecular and cellular biology. 2004; 24(12):5130–5143. [PubMed: 15169880]
62. Vertegaal AC, Andersen JS, Ogg SC, Hay RT, Mann M, Lamond AI. Distinct and overlapping sets of SUMO-1 and SUMO-2 target proteins revealed by quantitative proteomics. Mol Cell Proteomics. 2006; 5(12):2298–2310. [PubMed: 17000644]
63. Rodriguez MS, Dargemont C, Hay RT. SUMO-1 conjugation in vivo requires both a consensus modification motif and nuclear targeting. J Biol Chem. 2001; 276(16):12654–12659. [PubMed: 11124955]
64. Xue Y, Zhou F, Fu C, Xu Y, Yao X. SUMOsp: a web server for sumoylation site prediction. Nucleic Acids Res. 2006; 34:W254–W257. Web Server issue. [PubMed: 16845005]
65. Ren J, Gao X, Jin C, Zhu M, Wang X, Shaw A, et al. Systematic study of protein sumoylation: Development of a site-specific predictor of SUMOsp 2.0. Proteomics. 2009; 9(12):3409–3412.
66. Zhao Q, Xie Y, Zheng Y, Jiang S, Liu W, Mu W, et al. GPS-SUMO: a tool for the prediction of sumoylation sites and SUMO-interaction motifs. Nucleic Acids Res. 2014; 42:W325–W330. Web Server issue. [PubMed: 24880689]

67. Xu J, He Y, Qiang B, Yuan J, Peng X, Pan XM. A novel method for high accuracy sumoylation site prediction from protein sequences. BMC Bioinformatics. 2008; 9:8. [PubMed: 18179724]
68. Green, JR.; Dmochowski, GM.; Golshani, A. Can Med Biol Eng Conf. Vancouver, BC: 2006. Prediction of protein sumoylation sites via parallel cascade identification.
69. Thayer MM, Ahern H, Xing D, Cunningham RP, Tainer JA. Novel DNA binding motifs in the DNA repair enzyme endonuclease III crystal structure. EMBO J. 1995; 14(16):4108–4120. [PubMed: 7664751]
70. Kelley LA, Mezulis S, Yates CM, Wass MN, Sternberg MJE. The Phyre2 web portal for protein modeling, prediction and analysis. Nat Protocols. 2015; 10(6):845–858. [PubMed: 25950237]
71. Baba D, Maita N, Jee JG, Uchimura Y, Saitoh H, Sugasawa K, et al. Crystal structure of thymine DNA glycosylase conjugated to SUMO-1. Nature. 2005; 435(7044):979–982. [PubMed: 15959518]
72. Dizdaroglu M, Bauche C, Rodriguez H, Laval J. Novel substrates of Escherichia coli nth protein and its kinetics for excision of modified bases from DNA damaged by free radicals. Biochemistry. 2000; 39(18):5586–5592. [PubMed: 10820032]
73. Augeri L, Lee Y-M, Barton AB, Doetsch PW. Purification, characterization, gene cloning, and expression of *Saccharomyces cerevisiae* redoxyendonuclease, a homolog of *Escherichia coli* Endonuclease III. Biochemistry. 1997; 36(4):721–729. [PubMed: 9020769]
74. Boiteux S, Guillet M. Abasic sites in DNA: repair and biological consequences in *Saccharomyces cerevisiae*. DNA Repair. 2004; 3(1):1–12. [PubMed: 14697754]
75. Sedgwick B, Bates PA, Paik J, Jacobs SC, Lindahl T. Repair of alkylated DNA: recent advances. DNA Repair. 2007; 6(4):429–442. [PubMed: 17112791]
76. Swanson RL, Morey NJ, Doetsch PW, Jinks-Robertson S. Overlapping specificities of base excision repair, nucleotide excision repair, recombination, and translesion synthesis pathways for DNA base damage in Saccharomyces cerevisiae. Mol Cell Biol. 1999; 19(4):2929–2935. [PubMed: 10082560]
77. Gnad F, Gunawardena J, Mann M. PHOSIDA 2011: the posttranslational modification database. Nucleic Acids Res. 2011; 39:D253–D260. (Database issue). [PubMed: 21081558]
78. Rowe LA, Degtyareva N, Doetsch PW. DNA damage-induced reactive oxygen species (ROS) stress response in Saccharomyces cerevisiae. Free Radic Biol Med. 2008; 45(8):1167–1177. [PubMed: 18708137]
79. Jentsch S, Muller S. Regulatory Functions of Ubiquitin and SUMO in DNA Repair Pathways. Subcell Biochem. 2010; 54:184–194. [PubMed: 21222283]
80. Ho Y, Gruhler A, Heilbut A, Bader GD, Moore L, Adams SL, et al. Systematic identification of protein complexes in *Saccharomyces cerevisiae* by mass spectrometry. Nature. 2002; 415(6868): 180–183. [PubMed: 11805837]
81. Weinert TA, Kiser GL, Hartwell LH. Mitotic checkpoint genes in budding yeast and the dependence of mitosis on DNA replication and repair. Genes & development. 1994; 8(6):652–665. [PubMed: 7926756]
82. Noskov V, Maki S, Kawasaki Y, Leem SH, Ono B, Araki H, et al. The RFC2 gene encoding a subunit of replication factor C of Saccharomyces cerevisiae. Nucleic Acids Res. 1994; 22(9): 1527–1535. [PubMed: 8202350]
83. Boiteux S, Laval J. Mutagenesis by alkylating agents: coding properties for DNA polymerase of poly (dC) template containing 3-methylcytosine. Biochimie. 1982; 64(8–9):637–641. [PubMed: 6814512]
84. Larson K, Sahm J, Shenkar R, Strauss B. Methylation-induced blocks to in vitro DNA replication. Mutation research. 1985; 150(1–2):77–84. [PubMed: 4000169]
85. Prakash L. Lack of chemically induced mutation in repair-deficient mutants of yeast. Genetics. 1974; 78(4):1101–1118. [PubMed: 4376097]
86. Schwartz MF, Duong JK, Sun Z, Morrow JS, Pradhan D, Stern DF. Rad9 phosphorylation sites couple Rad53 to the Saccharomyces cerevisiae DNA damage checkpoint. Mol Cell. 2002; 9(5): 1055–1065. [PubMed: 12049741]

87. Toh GW, Lowndes NF. Role of the Saccharomyces cerevisiae Rad9 protein in sensing and responding to DNA damage. Biochemical Society transactions. 2003; 31(Pt 1):242–246. [PubMed: 12546694]

88. Conde F, Ontoso D, Acosta I, Gallego-Sanchez A, Bueno A, San-Segundo PA. Regulation of tolerance to DNA alkylating damage by Dot1 and Rad53 in Saccharomyces cerevisiae. DNA Repair (Amst). 2010; 9(10):1038–1049. [PubMed: 20674515]

89. Sarangi P, Bartosova Z, Altmannova V, Holland C, Chavdarova M, Lee SE, et al. Sumoylation of the Rad1 nuclease promotes DNA repair and regulates its DNA association. Nucleic Acids Res. 2014; 42(10):6393–6404. [PubMed: 24753409]

90. Hang LE, Lopez CR, Liu X, Williams JM, Chung I, Wei L, et al. Regulation of Ku-DNA association by Yku70 C-terminal tail and SUMO modification. J Biol Chem. 2014; 289(15): 10308–10317. [PubMed: 24567323]

91. Altmannova V, Eckert-Boulet N, Arneric M, Kolesar P, Chaloupkova R, Damborsky J, et al. Rad52 SUMOylation affects the efficiency of the DNA repair. Nucleic Acids Res. 2010; 38(14):4708–4721. [PubMed: 20371517]

92. Hardeland U, Steinacher R, Jiricny J, Schar P. Modification of the human thymine-DNA glycosylase by ubiquitin-like proteins facilitates enzymatic turnover. EMBO J. 2002; 21(6):1456–1464. [PubMed: 11889051]

93. Sacher M, Pfander B, Hoege C, Jentsch S. Control of Rad52 recombination activity by double-strand break-induced SUMO modification. Nat Cell Biol. 2006; 8(11):1284–1290. [PubMed: 17013376]

94. Steinacher R, Schar P. Functionality of human thymine DNA glycosylase requires SUMO-regulated changes in protein conformation. Curr Biol. 2005; 15(7):616–623. [PubMed: 15823533]

95. Bergink S, Ammon T, Kern M, Schermelleh L, Leonhardt H, Jentsch S. Role of Cdc48/p97 as a SUMO-targeted segregase curbing Rad51–Rad52 interaction. Nat Cell Biol. 2013; 15(5):526–532. [PubMed: 23624404]

96. Papouli E, Chen S, Davies AA, Huttner D, Krejci L, Sung P, et al. Crosstalk between SUMO and ubiquitin on PCNA is mediated by recruitment of the helicase Srs2p. Mol Cell. 2005; 19(1):123–133. [PubMed: 15989970]

97. Pfander B, Moldovan GL, Sacher M, Hoege C, Jentsch S. SUMO-modified PCNA recruits Srs2 to prevent recombination during S phase. Nature. 2005; 436(7049):428–433. [PubMed: 15931174]

98. Torres-Rosell J, Sunjevaric I, De Piccoli G, Sacher M, Eckert-Boulet N, Reid R, et al. The Smc5–Smc6 complex and SUMO modification of Rad52 regulates recombinational repair at the ribosomal gene locus. Nat Cell Biol. 2007; 9(8):923–931. [PubMed: 17643116]

99. Chen XL, Reindle A, Johnson ES. Misregulation of 2 microm circle copy number in a SUMO pathway mutant. Molecular and cellular biology. 2005; 25(10):4311–4320. [PubMed: 15870299]

Web References

100. http://www.abgent.com/sumoplot Date Last used: 8/4/16

Highlights

- Base excision repair (BER) proteins can be modified by SUMO
- Both *S. cerevisiae* Ntg1 and human NTHL1 can be sumoylated
- Five lysines are identified as the sites of SUMO modification in Ntg1
- An Ntg1 variant that cannot be modified by SUMO is generated
- Cells where Ntg1 cannot be modified by SUMO fail to respond properly to DNA damage

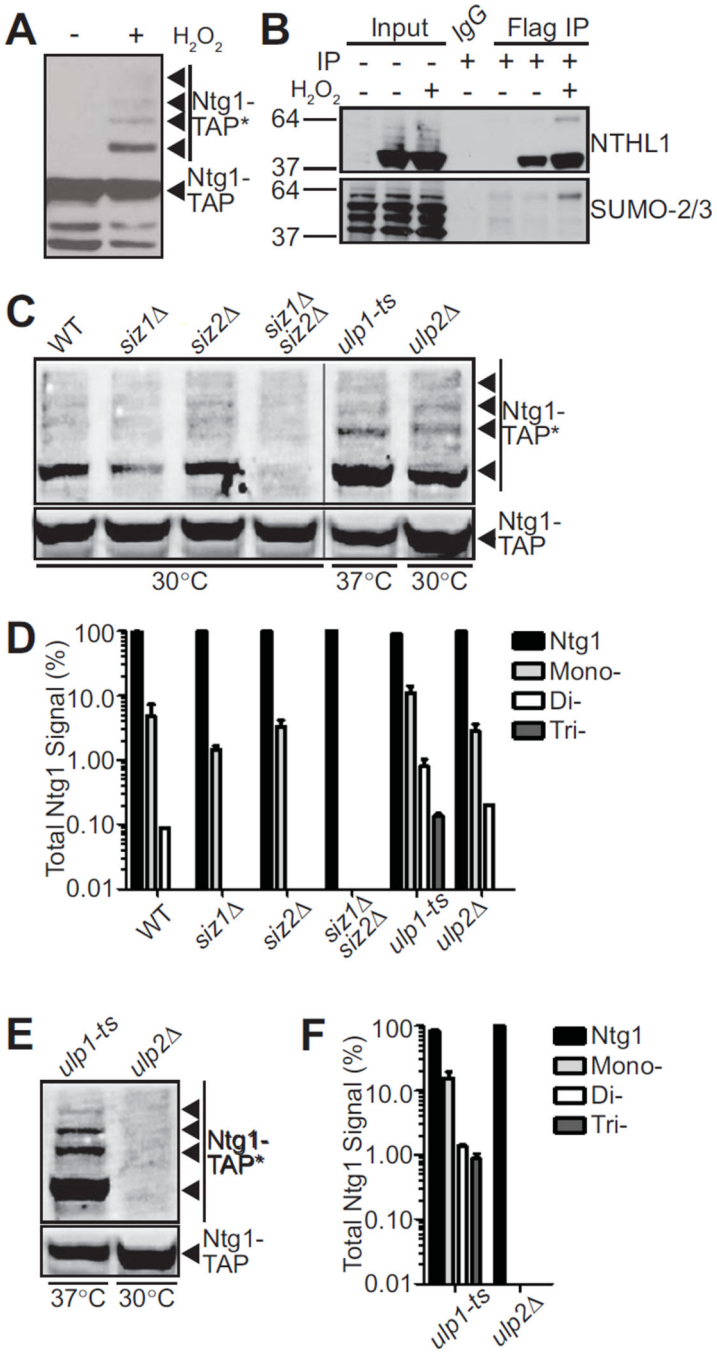

Figure 1. Sumoylation of Ntg1 is conserved and mediated by Siz1/2

A. Wildtype *S. cerevisiae* cells expressing Ntg1-TAP were exposed to 0 (−) or 20 mM (+) H_2O_2 for 1 hour at 30°C. Cells were pelleted, lysed, and immunoblotted to detect TAP-tagged Ntg1. Bands corresponding to post-translationally modified Ntg1 including SUMO-modified Ntg1 (24) are indicated by Ntg1-TAP*. **B.** Colon adenocarcinoma cells (HT29) were transfected with NTHL1-Flag or empty Flag vector and treated with 0 (−) or 125 μM (+) H_2O_2 for 15 minutes at 37°C. Cells were lysed, immunoprecipitated with Flag antibodies and both the Input and Flag IP fractions were subjected to immunoblotting. An IgG bead

alone immunoprecipitation was included as a control. The blot was probed with NTHL1 and SUMO-2/3 antibodies as indicated. **C.** Wildtype (WT), *siz1Δ, siz2Δ, siz1Δsiz2Δ, ulp1-ts,* or *ulp2Δ* cells were transformed with a plasmid expressing Ntg1-TAP. Cells were **(C)** exposed to 20 mM hydrogen peroxide or **(E)** not treated. Cells were incubated at 30°C except *ulp1-ts* cells which were shifted to the non-permissive temperature of 37°C. Each sample was lysed, immunoblotted, and bands were quantified. Nonadjacent lanes in the same image are separated by a black line. **D.** The data from **(C)** were quantitated. The total amount of Ntg1-TAP including unmodified and modified Ntg1-TAP was set to 100% (Ntg1) and the fraction of signal present in bands (Total Ntg1 Signal %) corresponding to the size consistent with Mono-, Di-, and Tri-sumoylation is plotted on a log scale. Results shown are the average of two independent experiments. Error bars represent SEM. **E.** To examine sumoylation of Ntg1 in the absence of oxidative damage, *ulp1-ts* and *ulp2Δ* cells expressing Ntg1-TAP were analyzed to detect any modified Ntg1 species (Ntg1-TAP*). **F.** The data from **(E)** were quantitated. The total amount of Ntg1-TAP including unmodified and modified Ntg1-TAP was set to 100% (Ntg1) and the fraction of signal present in bands (Total Ntg1 Signal %) corresponding to the size consistent with Mono-, Di-, and Tri-sumoylation is plotted on a log scale. Results shown are the average of two independent experiments. Error bars represent SEM.

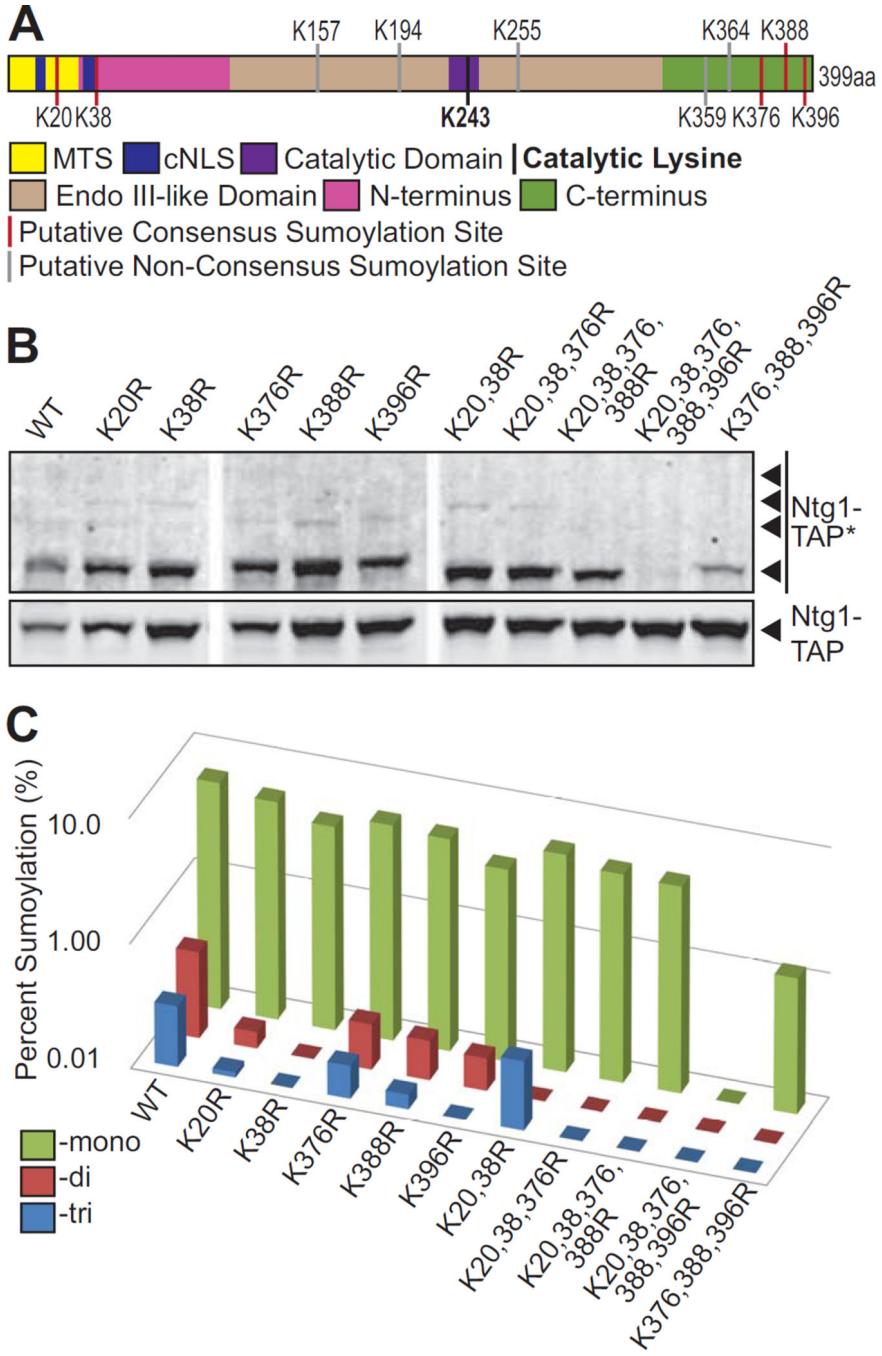

Figure 2. Identification of sumoylation sites in Ntg1

A. A domain schematic of Ntg1 is shown with the following functional motifs/domains indicated: The Mitochondrial Targeting Sequence (MTS) in yellow, the classical Nuclear Localization Signal (cNLS) in dark blue, the Catalytic Domain in purple. The Catalytic Lysine, K243, is depicted as a black bar. The central region of Ntg1 that is homologous to *E. coli* Endonuclease III is shown in tan (amino acids 95–335) while the non-conserved N- and C-terminal domains are indicted in magenta (amino acids 1–94) and green (amino acids 336–399), respectively. Putative Consensus Sumoylation Sites are shown as red bars and

Putative Non-Consensus Sumoylation Sites are shown as grey bars. **B.** A series of Ntg1 variants with candidate SUMO modification sites altered from lysine to arginine were generated and expressed in temperature sensitive *ulp1* cells. Cells were treated with 20 mM hydrogen peroxide for 1 hour at 30°C, lysed, and immunoblotted to detected Ntg1-TAP and modified Ntg1-TAP (Ntg1-TAP*). Nonadjacent lanes in the same image are separated by white space. **C.** Results from **(B)** were quantitated. For each Ntg1 variant, the percent of total Ntg1-TAP signal present in the band corresponding to the size of Mono-, Di-, and Tri-sumoylation (indicated as Percent Sumoylation) is plotted on a log scale.

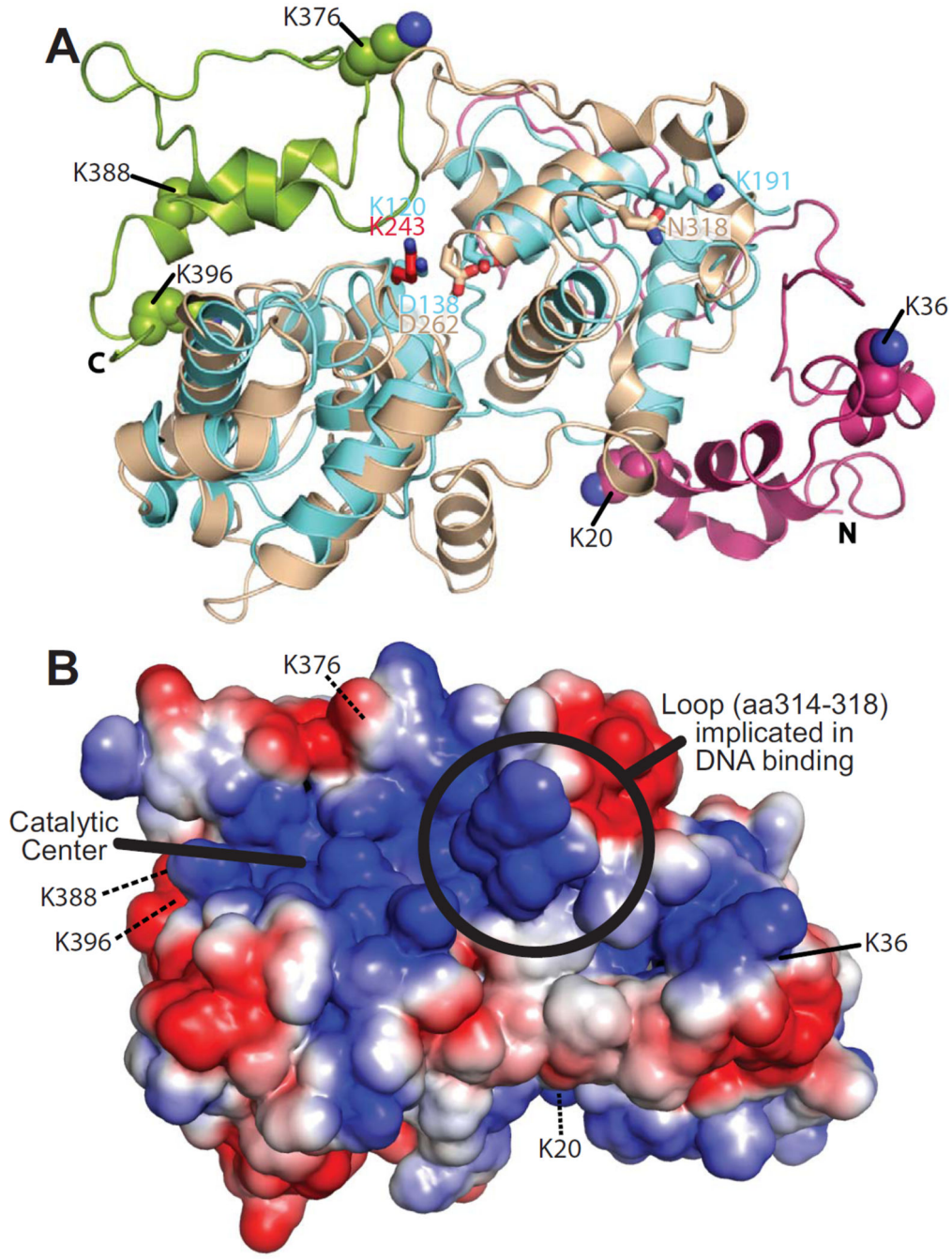

Figure 3. Homlogy model of Ntg1

A. A homology model of Ntg1 shown as a ribbon diagram was generated as described in Materials and Methods. The model is overlaid on the *E. coli* Ntg1 homologue, Endonuclease III, structure (cyan, PDB ID: 2ABK). The Ntg1 catalytic domain (amino acids 95–335; tan), N-terminal domain (amino acids 1–94; magenta), C-terminal domain (amino acids 336–399; green), catalytic amino acid of Ntg1 (K243, red) and Endonuclease III (K120, blue) are shown in addition to Endonuclease III amino acids D138, important for catalysis, and K191, implicated in DNA binding (69), and the corresponding amino acids in Ntg1 (D262 and

N318, respectively). The five consensus sumoylation sites (K20, K38, K376, K388, and K396) are shown as balls and indicated by the labeling. **B.** An electrostatic model of Ntg1 is shown based on the homology model. Positive and negative residues are colored in blue and red, respectively. White indicates neutral residues. The loop containing residues 314–318, indicated by a circle, has been implicated in DNA binding by Endo III (69). The catalytic center is indicated by a bold black line and the five consensus sumoylation sites are labeled and indicated by black lines. Residues 20, 376, 388, and 396 are located on the back face of the model and are indicated by black dotted lines.

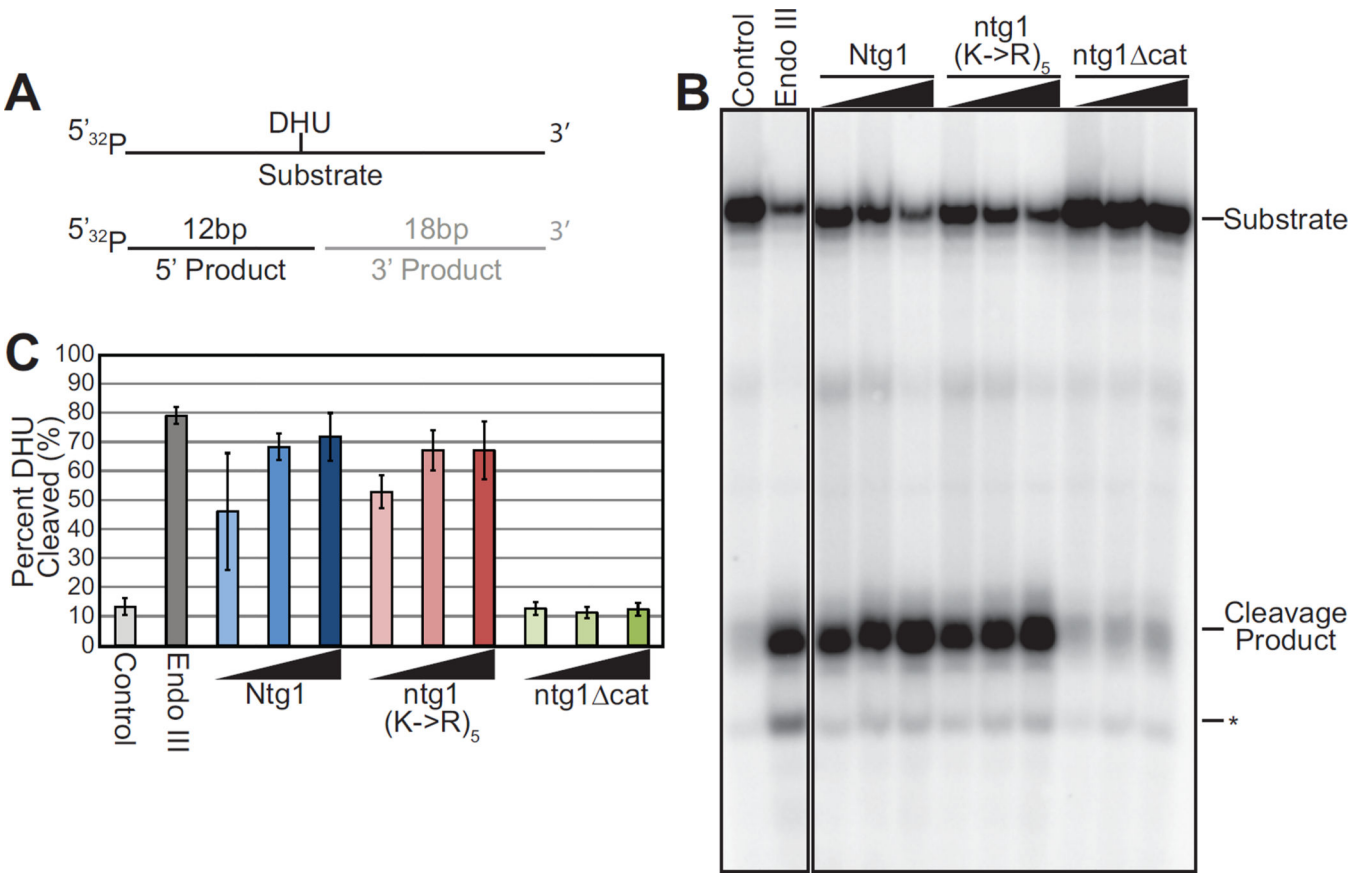

Figure 4. Functional analysis of Ntg1 variant

A. A schematic of the substrate employed for the *in vitro* cleavage assay, which contains dihydrouracil (DHU) embedded in a 31mer oligo, illustrating the substrate and expected products of the cleavage reaction is shown. **B.** Recombinant *E. coli* Endonuclease III (Endo III), and Ntg1 variants, His6-Ntg1, His6-ntg1(K->R)$_5$, catalytically inactive ntg1 (His6-ntg1Δcat), were employed for the *in vitro* cleavage assay. Increasing amounts of recombinant protein (5–50 ng) were added to radioactively-labeled substrate. Oligonucleotide Cleavage Products were electrophoresed and subjected to phosphorimager analysis. The Control lane shows the substrate with no added protein. The positive control is addition of 50 ng of *E. coli* Endo III. The position of the labeled product generated by cleavage (Cleavage Product) is indicated. Random degradation product is indicated by an asterisk (*). Nonadjacent lanes in the same image are separated by black lines. Results shown in **(B)** are representative of three independent experiments. **C.** Quantification of Cleavage Product generated for each Ntg1 variant from three independent experiments. Results are shown as Percent DHU Cleaved. Error bars represent standard deviation in the data.

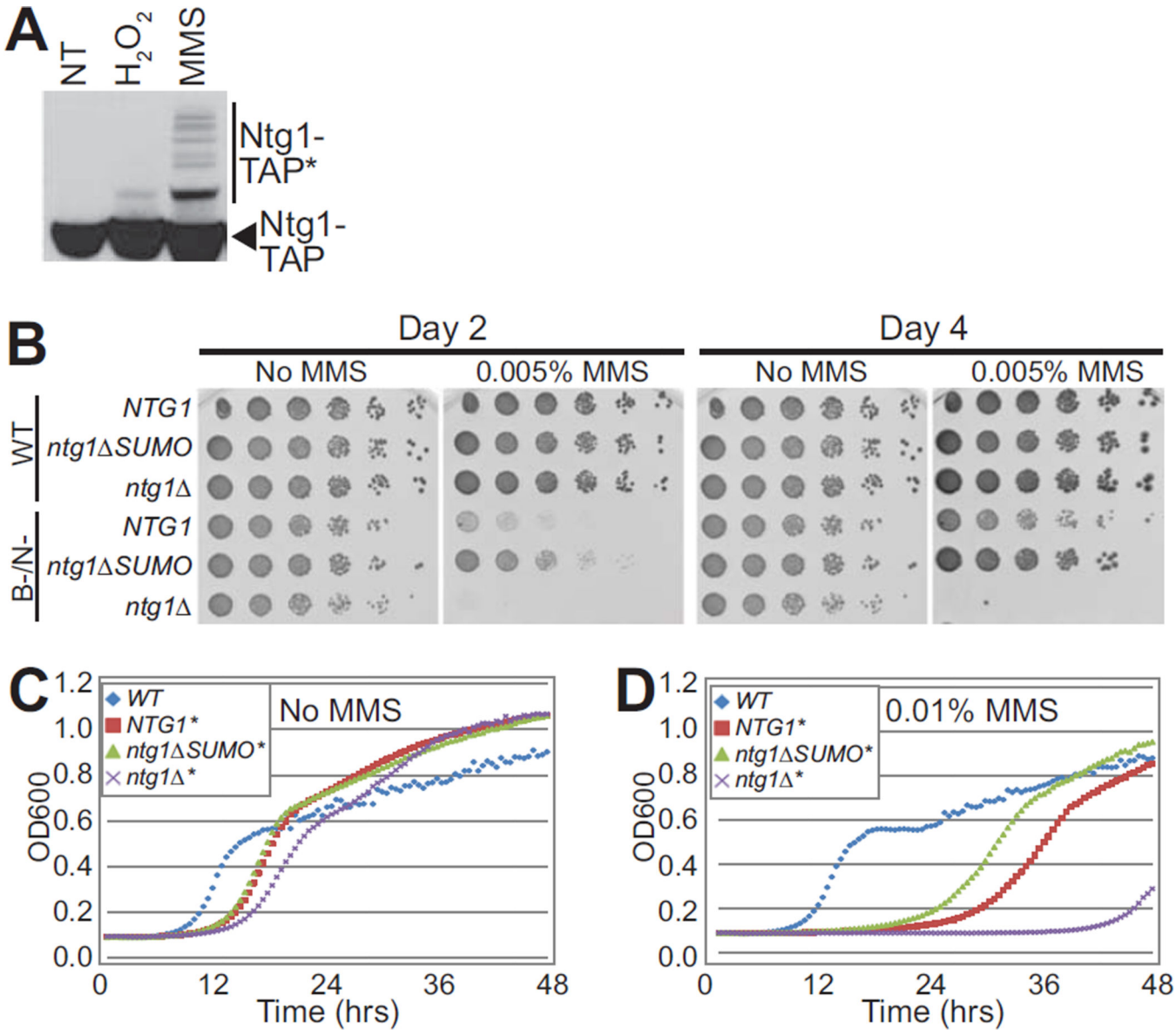

Figure 5. Functional analysis of ntg1ΔSUMO in DNA damage pathways

A. Wildtype cells expressing Ntg1-TAP were exposed to hydrogen peroxide (H_2O_2), methyl methanesulfonate (MMS), or were not treated (NT) and lysed. Lysate was subjected to immunoblotting to detect Ntg1-TAP and modified forms of Ntg1-TAP (Ntg1-TAP*). **B.** Cells with either a full complement of wildtype (WT) DNA repair pathways or deficient in both base excision repair and nucleotide excision repair (B-/N-) were employed. As described in Materials and Methods, the genotype for B-/N- cells (DSC0369) is *ntg1*Δ*ntg2*Δ*apn1*Δ*rad1*Δ. Both the WT and B-/N- cells were engineered to express ntg1ΔSUMO and compared to cells expressing NTG1 or lacking Ntg1 (*ntg1Δ*). Cultures were 5-fold serially diluted and spotted onto rich media or rich media containing 0.005% MMS and incubated at 30°C for 4 days. Pictures were taken at Day 2 and Day 4. **C/D.** The same samples as shown in **(B)** with either intact DNA repair pathways (WT) (blue diamond) or deficient in base excision repair and nucleotide excision repair (B-/N-), denoted by an *,

contain wildtype *NTG1* (red square), or *ntg1ΔSUMO* (green triangle), or lack Ntg1 (*ntg1Δ*) (purple X) at the endogenous *NTG1* locus. The genotype for B-/N- is *ntg1Δntg2Δapn1Δrad1Δ* (DSC0369). Cells were grown in liquid culture with No MMS **(C)** or with 0.01% MMS **(D)** for 48 hours. OD600 readings were taken every 30 minutes and plotted vs time. Results shown in **(B, C, and D)** are representative of at least three independent experiments.

Table 1

Strains and Plasmids Used in this Study

Strain or Plasmid	Description	References
DSC0295	*MAT***a***his3Δ1 leu2Δ0 met 15Δ0 ura3Δ0*; Tet-Off C-terminally TAP-tagged Ntg1	(24)
YSC1178-7499106 (DSC0297)	*MAT***a***his3Δ1 leu2Δ0 met15Δ0 ura3Δ0*; C-terminally TAP-tagged Ntg1	Open Biosystems
BY4147 (DSC0313)	*MAT***a***his3Δ1 leu2Δ0 met15Δ0 ura3Δ0*	Open Biosystems
DSC0470	*MAT***a** *ntg1::hphMX4, his7-1, lys2Δ5′::LEU-lys2Δ3′, ade5-1, trp1-289, ura3-52*	This study
EJY341 (DSC0527)	*MAT***a** *trp1-Δ1 ura3-52 his3-Δ200 leu2-3,112 lys2-801* [cir°]	(99)
EJY342 (DSC0528)	*MAT***a** *trp1-Δ1 ura3-52 his3-Δ200 leu2-3,112 lys2-801 siz1Δ::LEU2* [cir°]	(99)
EJY343 (DSC0529)	*MAT***a** *trp1-Δ1 ura3-52 his3-Δ200 leu2-3,112 lys2-801 siz2Δ::TRP1* [cir°]	(99)
EJY344 (DSC0530)	*MAT***a** *trp1-Δ1 ura3-52 his3-Δ200 leu2-3,112 lys2-801 siz1Δ::LEU2 siz2Δ::TRP1* [cir°]	(99)
MHY1488 (DSC0534)	*MAT***a** *ulp1Δ::HIS3 LEU2::ulp1-333*	(58)
EJY447 (DSC0535)	*MAT***a** *trp1-Δ1 ura3-52 his3-Δ200 leu2-3,112 lys2-801 ulp2Δ::kanMX* [cir°]	(60)
GBY5 (DSC0536)	*MAT***a** *smt3-allR::TRP1*	(55)
DSC0537	*MAT***a** *ntg1::hphMX4, his7-1, lys2Δ5′::LEU-lys2Δ3′, ade5-1, trp1-289, ura3-52,* pD0436	This study
DSC0538	*MAT***a** *trp1-Δ1 ura3-52 his3-Δ200 leu2-3,112 lys2-801* [cir°], pD0436	This study
DSC0539	*MAT***a** *smt3-allR::TRP1,* pD0436	This study
DSC0540	*MAT***a** *ulp1Δ::HIS3 LEU2::ulp1-333,* pD0436	This study
hDNP19	*MAT***a***/MATα rad1::kanMX/RAD1 ntg1::hphMX4/NTG1 ntg2::BSD/NTG2 apn1::TRP1/APN1 DSF1::URA3/DSF1 his7-1/his7-1 lys2Δ5′::LEU-lys2Δ3′/lys2Δ5′::LEU-lys2Δ3′ ade5-1/ade5-1 trp1-289/trp1-289 ura3-52/ura3-52*	(19)
DSC0367	*MAT***a** *his7-1 lys2Δ5′::LEU-lys2Δ3′ ade5-1 trp1-289 ura3-52*	(51)
DSC0369	*MAT***a** *ntg1::hphMX4* rad1::kanMX ntg2*::BSD apn1::TRP1 his7-1 lys2Δ5′::LEU-lys2Δ3′ ade5-1 trp1-289 ura3-52*	(51)
DSC0371	*MAT***a** rad1::kanMX ntg2*::BSD apn1::TRP1 his7-1 lys2Δ5′::LEU-lys2Δ3′ ade5-1 trp1-289 ura3-52*	(51)
DSC0561	*MAT***a** *ntg1*$_{k20,38,376,388,396R}$ rad1::kanMX ntg2*::BSD apn1::TRP1 DSF1::URA3 his7-1 lys2Δ5′::LEU-lys2Δ3′ ade5-1 trp1-289 ura3-52*	This study
DSC0549	*MAT***a** *ntg1*$_{k396R}$ rad1::kanMX ntg2*::BSD apn1::TRP1 DSF1::URA3 his7-1 lys2Δ5′::LEU-lys2Δ3′ ade5-1 trp1-289 ura3-52*	This study
DSC0551	*MAT***a** *ntg1*$_{k20,38R}$ rad1::kanMX ntg2*::BSD apn1::TRP1 DSF1::URA3 his7-1 lys2Δ5′::LEU-lys2Δ3′ ade5-1 trp1-289 ura3-52*	This study

Strain or Plasmid	Description	References
DSC0558	*MAT***a** *ntg1*$_{k20,38,376,388R}$ rad1.::kanMX ntg2*::BSD apn1*::*TRP1 DSF1*::*URA3 his7-1 lys2*Δ*5′*::*LEU-lys2*Δ*3′ ade5-1 trp1-289 ura3-52*	This study
DSC0561	*MAT***a** *ntg1*$_{k20,38,376,388,396R}$ rad1.::kanMX ntg2*::BSD apn1*::*TRP1 DSF1*::*URA3 his7-1 lys2*Δ*5′*::*LEU-lys2*Δ*3′ ade5-1 trp1-289 ura3-52*	This study
DSC0555	*MAT***a** *ntg1*$_{k376,388,396R}$ rad1.::kanMX ntg2*::BSD apn1*::*TRP1 DSF1*::*URA3 his7-1 lys2*Δ*5′*::*LEU-lys2*Δ*3′ ade5-1 trp1-289 ura3-52*	This study
pD0390	*pET-15b His6-NTG1*	(51)
pD0394	*pET -15b His6-NTG1*$_{\Delta cat}$	(51)
pD0493	*pET -15b His6-NTG1*$_{(K->R)5}$	This study
pD0436	Tet-Off NTG1-TAP, CEN, URA3, amp^R	This study
pD0437	Tet-Off ntg1$_{K20R}$-TAP, CEN, URA3, amp^R	This study
pD0438	Tet-Off ntg1$_{K38R}$-TAP, CEN, URA3, amp^R	This study
pD0444	Tet-Off ntg1$_{K376R}$-TAP, CEN, URA3, amp^R	This study
pD0445	Tet-Off ntg1$_{K388R}$-TAP, CEN, URA3, amp^R	This study
pD0446	Tet-Off ntg1$_{K396R}$-TAP, CEN, URA3, amp^R	This study
pD0447	Tet-Off ntg1$_{K20,38R}$-TAP, CEN, URA3, amp^R	This study
pD0448	Tet-Off ntg1$_{K20,38,376R}$-TAP, CEN, URA3, amp^R	This study
pD0449	Tet-Off ntg1$_{K20,38,396R}$-TAP, CEN, URA3, amp^R	This study
pD0450	Tet-Off ntg1$_{K20,38,376,388R}$-TAP, CEN, URA3, amp^R	This study
pD0451	Tet-Off ntg1$_{K20,38,376,388,396R}$-TAP, CEN, URA3, amp^R	This study
pD0452	Tet-Off ntg1$_{K376,388,396R}$-TAP, CEN, URA3, amp^R	This study

Table 2

Plasmid Construction Primers

Primer Purpose	Primer Name	Sequence (5' - 3')
pD0436	tetNtg1Cla-F1	GAATCGATTGCAGTTTCATTTGATGCTCGATGAG
	His-Ntg1Cla-R1	GAATCGATGTATTCTGGGCCTCCATGTCGC
K20R	K20R2-F	CAATTCTGAGGAAAAGACCGCTGGTAAGGACTGAAACTGG
	K20R2-R	CCAGTTTCAGTCCTTACCAGCGGTCTTTTCCTCAGAATTG
K38R	K38R-F	GGACCAAAATCAGACAAGAAGAGGTTGTCCCTCAACCCGTG
	K38R-R	CACGGGTTGAGGGACAACCTCTTCTTGTCTGATTTTGGTCC
K157R	K157R-F	GATGCTATCATCGCAAACAAGAGATGAAGTTACCGCAATGGC
	K157R-R	GCCATTGCGGTAACTTCATCTCTTGTTTGCGATGATAGCATC
K194R	K194R-F	CCGTTTTACAAATCAATGAGACCAGATTAGACGAATTGATTCATTCAG
	K194R-R	CTGAATGAATCAATTCGTCTAATCTGGTCTCATTGATTTGTAAAACGG
K255R	K255R-F	CATTACAAAAGGCATGGGGCAGGATTGAAGGTATCTGCGTTGACG
	K255R-R	CGTCAACGCAGATACCTTCAATCCTGCCCCATGCCTTTTGTAATG
K359R	K359R-F	GCAAAATATCATGAGTTATCCAAAGTGGGTGAGATACCTGGAAGG
	K359R-R	CCTTCCAGGTATCTCACCCACTTTGGATAACTCATGATATTTTGC
K364R	K364R-F	TACCTGGAAGGAAGACGTGAACTGAACGTGGAGGCGG
	K364R-R	CCGCCTCCACGTTCAGTTCACGTCTTCCTTCCAGGTA
K376R	K376R-F	CGTGGAGGCGGAAATCAATGTTAGACACGAGGAGAAAACAG
	K376R-R	CTGTTTTCTCCTCGTGTCTAACATTGATTTCCGCCTCCACG
K388R	K388R-F	CGAGGAGAAAACAGTTGAAGAAACTATGGTCAGACTGGAAAATG
	K388R-R	CATTTTCCAGTCTGACCATAGTTTCTTCAACTGTTTTCTCCTCG
K396R	K396R-F	GGAAAATGATATTTCTGTTAGAGTAGAGGACGGTCGACGG
	K396R-R	CCGTCGACCGTCCTCTACTCTAACAGAAATATCATTTTCC
NTHL1	NTHL1-Flag-F	ACACTGGCGGCCGTTACTAGTGGATCCT
	NTHL1-Flag-R	ACGACTCACTATAGGGAGACCCAAGCTT

Table 3

Quantification of Mono-, Di-, Tri- Sumoylation of Ntg1 Variants

Potential Sumo Modification	Fraction of Modified Ntg1 (%)										
	WT	**K20R**	**K38R**	**K376R**	**K388R**	**K396R**	**K20, 38R**	**K20,38, 376R**	**K20,38, 376, 388R**	**K20,38, 376,388, 396R**	**K376, 388, 396R**
Ntg1-Tri	0.31	0.11	0.02	0.18	0.13	0.00	0.36	0.02	0.00	0.00	0.00
Ntg1-Di	0.49	0.14	0.00	0.23	0.21	0.18	0.00	0.05	0.00	0.00	0.00
Ntg1-Mono	6.52	5.53	4.27	5.30	4.98	3.45	5.50	4.66	4.51	0.04	1.24

DNA Repair (Amst). Author manuscript; available in PMC 2017 December 01.